Bayesian analysis of rare events

3 authors:

Daniel Straub
Technische Universität München
214 PUBLICATIONS **2,759** CITATIONS

SEE PROFILE

Iason Papaioannou
Technische Universität München
71 PUBLICATIONS **674** CITATIONS

SEE PROFILE

Wolfgang Betz
Technische Universität München
20 PUBLICATIONS **290** CITATIONS

SEE PROFILE

Some of the authors of this publication are also working on these related projects:

Project   Reliability of hydraulic structures considering spatial variability View project

Project   SAFEPEC - Innovative, risk-based inspection for a smarter and safer waterborne industry View project

Bayesian analysis of rare events

Daniel Straub, Iason Papaioannou, Wolfgang Betz

Engineering Risk Analysis Group, Technische Universität München (straub@tum.de, www.era.bgu.tum.de)

Abstract

In many areas of engineering and science there is an interest in predicting the probability of rare events, in particular in applications related to safety and security. Increasingly, such predictions are made through computer models of physical systems in an uncertainty quantification framework. Additionally, with advances in IT, monitoring and sensor technology, an increasing amount of data on the performance of the systems is collected. This data can be used to reduce uncertainty, improve the probability estimates and consequently enhance the management of rare events and associated risks. Bayesian analysis is the ideal method to include the data into the probabilistic model. It ensures a consistent probabilistic treatment of uncertainty, which is central in the prediction of rare events, where extrapolation from the domain of observation is common. We present a framework for performing Bayesian updating of rare event probabilities, termed BUS. It is based on a reinterpretation of the classical rejection-sampling approach to Bayesian analysis, which enables the use of established methods for estimating probabilities of rare events. By drawing upon these methods, the framework makes use of their computational efficiency. These methods include the First-Order Reliability Method (FORM), tailored importance sampling (IS) methods and Subset Simulation (SuS). In this contribution, we briefly review these methods in the context of the BUS framework and investigate their applicability to Bayesian analysis of rare events in different settings. We find that, for some applications, FORM can be highly efficient and is surprisingly accurate, enabling Bayesian analysis of rare events with just a few model evaluations. In a general setting, BUS implemented through IS and SuS is more robust and flexible.

Keywords

Rare events; reliability; Bayesian analysis; importance sampling; subset simulation.

1 Introduction

The probability of rare events is of interest in many physical systems. Examples include the probability of infrastructure system failures (Duenas-Osorio and Vemuru 2009), the probability of failure of technical systems in general (Bedford and Cooke 2001), probabilities of extreme natural hazard events (Cornell 1968), or probabilities of extreme climate developments (Dessai and Hulme 2004). The optimal management of such adverse rare events is strongly facilitated by the availability of accurate probability assessments. Purely statistical methods are often not sufficient for this task, due to the uniqueness of the considered systems and the fact that accurate estimation of rare event probabilities requires large datasets (Straub 2014). An alternative is the assessment of rare events through the use of physical models, in combination with probabilistic models of the relevant model parameters. In physical systems, uncertainty is present in material and geometrical properties, environmental factors and the models themselves. By modeling these uncertainties probabilistically and propagating them through the physical models, a probabilistic description of the model output is obtained.

Methods for computing the probability of rare events based on physical and engineering models have been developed since the 1970s in the field of structural reliability (Rackwitz and Fiessler 1978, Der Kiureghian and Liu 1986). Methodological developments were motivated by the demand for rational approaches to dealing with uncertainty in the design of structural systems, which have high requirements to their safety. For structures and other safety-critical technical systems, requirements to the probability of failure are in the order of $10^{-4} - 10^{-6}$ during the lifetime of the system, or as low as 10^{-8} during one hour of operation (Paté-Cornell 1994). The computation of such small probabilities through the use of probabilistic physical models corresponds to an extrapolation, and the resulting probabilities must be interpreted carefully, a fact that is well appreciated by experts in structural reliability (Melchers 1999).

To improve the estimates of rare event probabilities, data obtained on the actual system, e.g., through monitoring systems or measurement campaigns, can provide useful information on the potential rare event. As an example, in geotechnical engineering, the observational method is commonly used to limit the risk of catastrophic failures (Peck 1969). To systematically and quantitatively include such data into rare event probabilities, Bayesian analysis provides an optimal framework. Often, data is available on the input parameters to the model of the system. In these cases, Bayesian analysis can be used to learn (update) their probability distributions (Gelman 2004). This corresponds to a classical statistical analysis, and we will not further go into this. We focus on systems where data is available on the system response. In these cases, Bayesian analysis is commonly used as a technique to solve the inverse problem of determining

probabilistically the input parameters given output data. It is e.g. applied to the solution of inverse problems in subsurface flow (Elsheikh et al. 2014), structural identification (Beck and Katafygiotis 1998) or hydrology (Kavetski et al. 2006), to name just a few examples.

When the interest is in the probability of rare events conditional on the data, it is possible to first perform a Bayesian analysis to learn the probability distribution of the input parameters, and then apply these updated distributions to the prediction of the rare events. Such an approach has e.g. been pursued in (Papadimitriou et al. 2001, Jensen et al. 2013, Sundar and Manohar 2013, Hadjidoukas et al. 2015). The resulting conditional probability is often termed the *posterior robust failure probability* in the literature. (The word *robust* is avoided in this paper, as it implies explicit modeling of the model uncertainties through multiple model classes (Papadimitriou et al. 2001), which is not considered here.) The difficulty in estimating the posterior failure probability lies in the fact that the rare event probability cannot be efficiently estimated using a crude Monte Carlo simulation approach. Therefore, the method for Bayesian inverse analysis must be combined with a separate efficient method for evaluating rare event probabilities. Most of these methods require explicit knowledge of the joint (posterior) probability distribution of the random variables, which must thus be approximated from the posterior samples. This approximation can cause significant errors.

In contrast to these approaches, we develop a framework that enables the computation of the posterior distribution and the conditional probability of the rare event with a single method. This has the advantage that it is not required to employ an approximate posterior distribution as an input to a posterior rare event probability estimation. This is achieved by combining the simple but ineffective rejection sampling approach to Bayesian analysis with structural reliability methods (SRM). For this reason it is termed BUS (Bayesian Updating with SRM). Besides its simplicity, the framework can potentially lead to computational benefits over existing approaches, since it enables the use of all existing SRM for this task. In (Straub and Papaioannou 2015), we proposed BUS for learning the posterior distribution of the input variables. Here, we show that it is ideally suited for Bayesian analysis of rare events and present its implementation.

The paper starts out with an introduction to the estimation of rare event probabilities through classical SRM, in particular the first-order reliability method (FORM). This is followed by a short review of possible approaches to computing the updated rare event probability. We then introduce the BUS methodology for rare events and its implementation with three SRM: FORM, line sampling and subset simulation. Finally, the methodology is illustrated and investigated through four numerical examples.

2 Methodology

2.1 Computing probabilities of rare events: Structural reliability methods

For efficiently estimating the probability of rare events, a class of methods called Structural Reliability Methods (SRM) has been developed since the 1970s (e.g., Rackwitz and Fiessler 1978, Der Kiureghian and Liu 1986). The following briefly introduces the basic concepts of SRM; comprehensive introductions can be found in (Ditlevsen and Madsen 1996, Melchers 1999).

In SRM, the rare event of interest, typically the failure event F, is described in terms of a so-called limit state function $g(\mathbf{X})$, where $\mathbf{X} = [X_1; X_2; \dots; X_n]$ is the vector of the n input random variables of the problem. By definition, the event F corresponds to

$$F = \{g(\mathbf{X}) \leq 0\} \tag{1}$$

It is helpful to interpret the SRM geometrically: Ω_F corresponds to the domain in the outcome space of $\mathbf{X}$ for which $g(\mathbf{x}) \leq 0$. The probability of the event F is the probability of $\mathbf{X}$ taking a value within Ω_F. It can be computed by integrating the joint probability density function of $\mathbf{X}$, denoted by $f_{\mathbf{X}}(\mathbf{x})$, over Ω_F:

$$\Pr(F) = \int_{g(\mathbf{x}) \leq 0} f_{\mathbf{X}}(\mathbf{x}) \mathrm{d}x_1 \mathrm{d}x_2 \dots \mathrm{d}x_n \tag{2}$$

The problem is illustrated in Figure 1a. For the case of two random variables, as in Figure 1a, numerical integration is straightforward, e.g. using adaptive quadrature rules that resolve the boundary of Ω_F. However, most classical methods for numerical integration have computation times that increase exponentially with the number of dimensions, and are therefore not suitable for solving Eq. (2) for realistic applications with larger values of n.

All SRM aim at solving Eq. (2), and each method has its specific advantages and disadvantages. Most SRM involve a transformation of the problem from the original space of the random variables $\mathbf{X}$ to the space of independent standard normal random variables $\mathbf{U}$ by a suitable transformation $\mathbf{U} = \mathbf{T}(\mathbf{X})$. If the $\mathbf{X}$ are (a-priori) mutually independent, the transformation is simply

$$U_i = \Phi^{-1}\big[F_{X_i}(X_i)\big], i = 1, \dots, n \tag{3}$$

where F_{X_i} is the marginal cumulative distribution function (CDF) of X_i and Φ^{-1} is the inverse standard normal CDF. If the joint distribution of **X** is of the Gaussian copula class, the Nataf transformation can be applied (Der Kiureghian and Liu 1986); if the joint distribution of **X** is of any arbitrary form, the Rosenblatt transformation can be used (Rosenblatt 1952, Hohenbichler and Rackwitz 1981). The reader is referred to (Ditlevsen and Madsen 1996) and (Melchers 1999) for details.

Probabilistic transformation techniques require the joint distribution of **X** to be known explicitly. That is, any arbitrary distribution can be transformed to standard normal space, provided that the distribution is known. For cases where the distribution of **X** is not known in explicit form and thus such a transformation is not possible, there exist SRM that can be applied directly in the original random variable space. Hence, the probabilistic transformation step is not a strict requirement for further developments. However, in most practical situations the distribution of **X** is known and the probabilistic transformation is straightforward. Moreover, the performance of most SRM can benefit from an implementation in the **U**-space.

Let G denote the transformed limit state function in standard normal space:

$$G(\mathbf{U}) = g(\mathbf{T}^{-1}(\mathbf{U})) \tag{4}$$

where $\mathbf{T}^{-1}(\mathbf{U}) = \mathbf{X}$ is the inverse transformation from standard normal space to the original outcome space of the random variables. The transformation **T** is probability conserving, therefore $\Pr(F) = \Pr(g(\mathbf{X}) \leq 0) = \Pr(G(U) \leq 0)$. In analogy to Eq. (2), the probability of the failure event F is now computed by

$$\Pr(F) = \int_{G(\mathbf{u}) \leq 0} \varphi(\mathbf{u}) \mathrm{d}u_1 \mathrm{d}u_2 \dots \mathrm{d}u_n, \tag{5}$$

where φ is the multivariate independent standard normal probability density function (PDF). The transformation of the limit state surface $g(\mathbf{x}) = 0$ to the corresponding surface in standard normal space $G(\mathbf{u}) = 0$ is illustrated in Figure 1.

2.1.1 Structural reliability methods based on the most likely failure point

The most well-known SRM is the First-Order Reliability Method (FORM), which approximates the limit state function $G(\mathbf{U})$ by a first-order Taylor expansion at the expansion point $\mathbf{u}^*$, denoted by $G'(\mathbf{U})$. To limit the approximation error, $\mathbf{u}^*$ is selected as the point in the failure

domain with the highest probability density, the so-called most likely failure point or design point[1]. Because the standard multivariate normal PDF φ is rotation-symmetric around the origin, the design point $\mathbf{u}^*$ is equal to the point on the failure surface $G(\mathbf{U}) = 0$ that is the closest to the origin. The identification of the expansion point therefore corresponds to a constrained (geometrical) minimization problem:

$$\begin{aligned} \mathbf{u}^* &= \arg\min\|\mathbf{u}\| \\ &\text{subject to } G(\mathbf{u}) = 0, \end{aligned} \tag{6}$$

where $\|\mathbf{u}\| = \sqrt{\mathbf{u}^\mathrm{T}\mathbf{u}}$ is the distance of $\mathbf{u}$ from the origin.

With this approximation, the limit state surface is approximated by its tangent at the design point, see Figure 1b. In FORM, the integration over the domain $\{G(\mathbf{u}) \leq 0\}$ is thus replaced by the integration over a half space defined by the tangent $\{G'(\mathbf{u}) = 0\}$. Every marginal distribution of the multivariate independent standard normal distribution is a standard normal distribution. Therefore, the marginal probability distribution of $\mathbf{U}$ in the direction perpendicular to the linearized limit state surface is also a standard normal distribution, as illustrated in Figure 1. The FORM approximation of the probability of failure is fully defined by the distance $\beta_{\mathrm{FORM}} = \|\mathbf{u}^*\|$ between the origin and the design point as

$$\Pr(F) \approx \Pr(G'(\mathbf{U}) \leq 0) = \Phi(-\beta_{\mathrm{FORM}}) \tag{7}$$

where Φ is the standard normal cumulative distribution function (CDF). β_{FORM} is known as the FORM reliability index[2].

The computational bottleneck of FORM is the identification of the design point $\mathbf{u}^*$, i.e. the solution of the optimization problem of Eq. (6). Tailored algorithms exist for this purpose (Liu and Der Kiureghian 1991). Since these are gradient-based methods, the computational cost of the optimization increases with increasing number of dimensions n. Specialized response surface methods have been developed to limit the number of calls of the function $g(\mathbf{X})$, e.g.

---

[1] The term design point originates from the fact that $\mathbf{x}^* = \mathbf{T}^{-1}(\mathbf{u}^*)$ are the parameter values that are ideally used in a deterministic design calculation, in order to capture the likely failure configuration, see (Melchers 1999).

[2] If the limit state function is negative at the origin $\mathbf{0}$, then $\beta_{\mathrm{FORM}} = -\|\mathbf{u}^*\|$ and the FORM estimate is larger than 0.5. In such cases, however, FORM should not be applied.

(Bucher and Bourgund 1990, Sudret 2012), but their performance also deteriorates with increasing dimensions.

(a) original variable space   **(b) standard normal space**
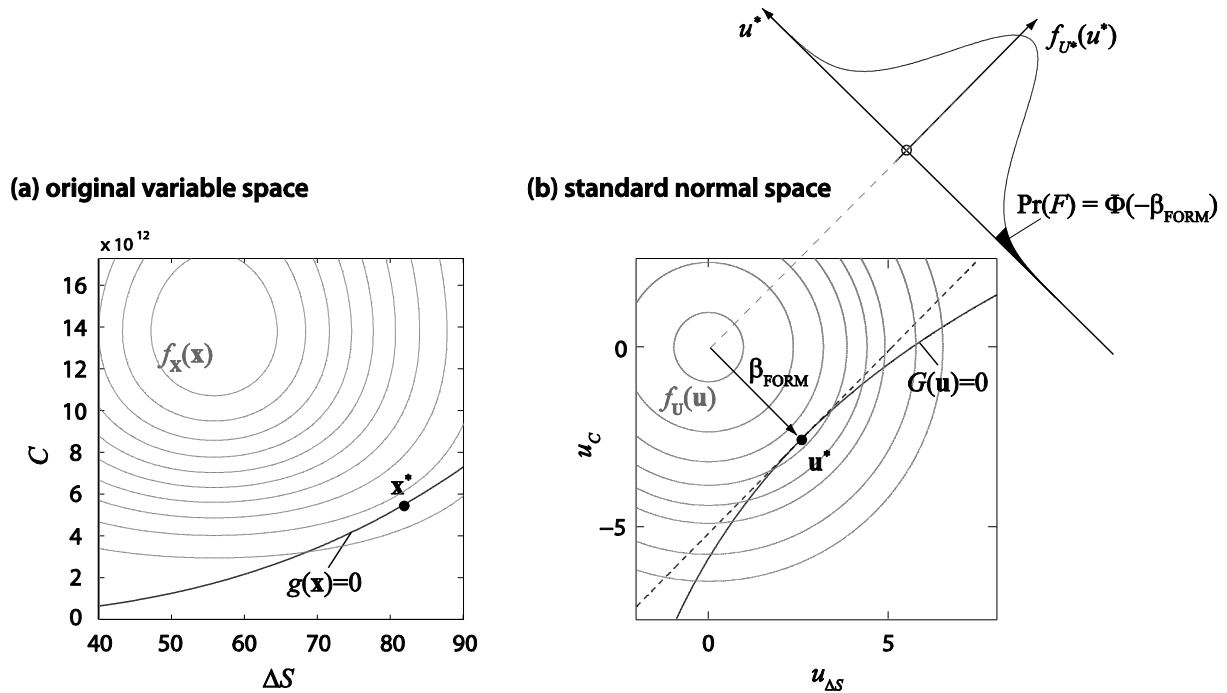
*Figure 1. Design point and linear approximation of the limit state surface. Left side: original random variable space; right side: standard normal space. The marginal distribution of **U** in the direction of the design point **u*** is the standard normal distribution. Hence the FORM approximation of the failure probability is given by Eq. (7). [Details of this example are provided in (Straub 2014).]*

Once the design point is identified, FORM is surprisingly accurate for a wide range of problems (Rackwitz 2001). However, the approximation error is difficult to estimate, and it is often beneficial to check and improve the accuracy of FORM by a second-order approximation around the design point (Breitung 1984). As a general rule, the accuracy of FORM decreases with increasing dimensions n, but many high-dimensional problems can be handled by suitable dimensionality-reduction techniques, see e.g. (Allaix and Carbone 2015) for the coupling of FORM with a Karhunen–Loève expansion. Additionally, specific techniques for importance sampling around the design point have been developed, some of which also work in high dimensions. One of these techniques, line sampling, is introduced later.

2.1.2   Sampling-based structural reliability methods

A large number of sampling-based SRM exist for estimating the probability of rare events. These include a variety of importance sampling (IS) techniques that aim at a reduction of the variance of standard Monte Carlo probability estimates. The efficiency of IS highly depends on the choice of the sampling density. Common choices are unimodal IS densities centered in the

design point obtained from a preliminary FORM analysis (Schuëller and Stix 1987). Alternatively, adaptive IS techniques that do not require knowledge of the design point are popular (Bucher 1988, Engelund and Rackwitz 1993, Au and Beck 1999). In this category, cross-entropy-based IS schemes have recently been proposed for rare event estimation (Botev et al. 2007, Li et al. 2011, Kurtz and Song 2013), as well as sequential IS (Papaioannou et al. 2014). To enhance the efficiency of IS methods, importance sampling schemes have been combined with response surface approaches (surrogate models) (Bucher and Bourgund 1990, Paffrath and Wever 2007, Li and Xiu 2010, Li et al. 2011).

An importance sampling approach that enables efficient estimation of the probability of rare events is the line sampling method (Hohenbichler and Rackwitz 1988, Rackwitz 2001, Koutsourelakis et al. 2004). Line sampling generates samples on a hyperplane orthogonal to an important direction pointing to the limit state surface. The direction can be chosen as the one pointing to the design point or based on the results from an initial Monte Carlo simulation. The method is shown to be efficient in problems with a large number of random variables n (Pradlwarter et al. 2007). Line sampling will be utilized later in this paper and is described in Section 3.2.

In recent years, Subset Simulation (SuS) proposed in (Au and Beck 2001) has become a popular SRM. It belongs to the family of sequential Monte Carlo methods (Del Moral et al. 2006, Cérou et al. 2012). In contrast to standard IS with unimodal or multimodal IS densities, the performance of SuS is not directly dependent on the number of input random variables n (Schuëller et al. 2004, Katafygiotis and Zuev 2007). SuS has also been combined with surrogate models (e.g., Bourinet et al. 2011). A short summary of SuS is provided in Section 3.3.

2.2 Bayesian analysis of rare events

In many instances, data $\mathbf{d}$ is available, which provides information directly or indirectly on the random variables $\mathbf{X}$ in the limit state function. In a Bayesian setting, the data is used to update the prior probability distribution $f_{\mathbf{X}}$ to a posterior distribution $f_{\mathbf{X}|\mathbf{d}}$:

$$f_{\mathbf{X}|\mathbf{d}}(\mathbf{x}) \propto L(\mathbf{x}) f_{\mathbf{X}}(\mathbf{x}) \tag{8}$$

$L(\mathbf{x}) = f_{\mathbf{D}|\mathbf{X}}(\mathbf{d}|\mathbf{x})$ is the likelihood function describing the data. Note that the data may not provide information on all random variables in $\mathbf{X}$. For example, one can distinguish between uncertain model parameters, which can be learned, and uncertain future forcing variables, which cannot be learned. In the following, we do not make this distinction, and note that the

likelihood function is simply constant with respect to all random variables in **X** on which the data contains no information.

Conversely, in some cases the likelihood can only be explicitly formulated as a function of additional input random variables that do not affect the limit state function g. This is e.g. the case in dynamic systems, in which the data are measurements of system responses that are a function of possibly uncertain forcing variables. In such situations, the vector **X** is augmented by these random variables. In principle it is possible to separate these variables within the framework (e.g. following (Beck 2010)), and this may have implications on the computational efficiency (Hadjidoukas et al. 2015). However, for ease of presentation we here choose to not make this distinction and include in **X** all random variables that are arguments of the likelihood function.

The probability of the rare event conditional on the data, i.e. the posterior failure probability, is obtained by inserting the posterior $f_{\mathbf{X}|\mathbf{d}}(\mathbf{x})$ into Eq. (2):

$$
\Pr(F|\mathbf{d}) = \int_{g(\mathbf{x}) \leq 0} f_{\mathbf{X}|\mathbf{d}}(\mathbf{x}) \, dx_1 dx_2 \dots dx_n \tag{9}
$$

In the general case, only an approximation of the posterior PDF $f_{\mathbf{X}|\mathbf{d}}$ or CDF $F_{\mathbf{X}|\mathbf{d}}$ is available, typically through samples of $f_{\mathbf{X}|\mathbf{d}}$. Most SRM have difficulties in working with such an approximation, which might limit the efficiency in determining $\Pr(F|\mathbf{d})$. One exception is SuS, which is employed in (Jensen et al. 2013, Hadjidoukas et al. 2015) for evaluating Eq. (9) starting from samples of the posterior. However, it is often efficient to apply SuS in standard normal space, as discussed in (Papaioannou et al. 2015), which requires explicit knowledge of $f_{\mathbf{X}|\mathbf{d}}$.

For these reasons, there is a benefit in developing a framework that does not required solving Eq. (9) based on samples of the posterior, but enables a computation of the posterior failure probability $\Pr(F|\mathbf{d})$ directly within the framework of SRM. Already in the 1980s, such a concept was proposed, which has similarities with the ABC method, as reviewed in the next section. A novel framework, which does not require the approximation made by ABC, is then presented in Section 2.4.

2.3 ABC and early methods for updating structural reliability

In recent years, Approximate Bayesian Computation (ABC) has become a popular approach for performing Bayesian analysis. It circumvents the explicit formulation of a likelihood function

and can handle potentially large numbers of uncertain parameters and data. Consider measurements $\mathbf{d}$ that correspond to model outputs $q(\mathbf{X})$. With additive measurement errors $\boldsymbol{\epsilon}$, the likelihood function is $L(\mathbf{x}) = f_\epsilon[\mathbf{d} - q(\mathbf{x})]$, but alternatively these measurements can be described by the equality $\mathbf{d} = q(\mathbf{x}) + \epsilon$. ABC is a sampling-based method that can be summarized as follows[3]: Applying a simple acceptance/rejection algorithm, hypothetical data $\hat{\mathbf{d}}(\mathbf{x})$ are generated based on sampling of $\mathbf{X}$ and $\boldsymbol{\epsilon}$ from their respective prior distribution. A performance metric ρ is formulated, which gives a measure of the "distance" from $\hat{\mathbf{d}}(\mathbf{x})$ to the actually observed data $\mathbf{d}$. Samples of $\mathbf{X}$ are then accepted if their ρ is within a certain tolerance limit τ:

$$\rho\big(\hat{\mathbf{d}}(\mathbf{x}), \mathbf{d}\big) \leq \tau \tag{10}$$

For details on the performance measures and for more efficient versions of the sampling algorithms, the reader is referred to the extensive ABC literature, e.g. (Beaumont et al. 2009, Csilléry et al. 2010, Fearnhead and Prangle 2012, Marin et al. 2012)

In the structural reliability community, a related approach had been proposed for Bayesian updating of the probability of failure already in the 1980s (Madsen et al. 1985, Madsen 1987, Schall et al. 1989). By including measurement errors explicitly as random variables $\boldsymbol{\epsilon}$, the data was described through functions h_i in analogy to the limit state function g. For a data point d, the function would be $h(\mathbf{x}) = \hat{d}(\mathbf{x}) - d$, and it is required that $h(\mathbf{x}) = 0$. This corresponds to setting a tolerance $\tau = 0$ in Eq. (10). In the structural reliability context, $Z = \{h(\mathbf{X}) = 0\}$ is defined as an observation event, and $\Pr(F|Z) = \Pr(F|d)$ is estimated by first- or second-order approximations of surface integrals (Schall et al. 1989).

These methods did not gain much attention, because the error associated with the first-order approximation increases with increasing amount of data, and the concept is incompatible with sampling-based SRM due to the inability of sampling methods to produce estimates of surface integrals (Sindel and Rackwitz 1998). However, by observing the strong analogy to ABC, the approach can be reformulated in a way that facilitates the use of sampling-based SRM. Both approaches circumvent the likelihood function by explicitly introducing measurement errors $\boldsymbol{\epsilon}$ as random variables in the formulation. In the outcome space of the random variables $\mathbf{X}$ and $\boldsymbol{\epsilon}$,

---

[3] The notation here differs from the standard notation used in the ABC literature, to be consistent with the remainder of this paper. In the ABC literature, ϵ commonly denotes the tolerance instead of τ used here, θ denotes the random variables instead of $\mathbf{X}$.

the observations then correspond to a lower-dimensional surface. Casting the ABC approach in the structural reliability framework, the performance function can be defined as $|h(\mathbf{x}, \boldsymbol{\epsilon})|$ and the approximate observation domain written as:

$$Z = \{|h(\mathbf{X}, \boldsymbol{\epsilon})| \leq \tau\} \tag{11}$$

The probability of this approximate observation event is a domain integral, and hence sampling methods are applicable. (Chiachio et al. 2014) have proposed such an approach for learning model parameters through ABC with SuS.

2.4 Bayesian analysis in a structural reliability framework: the BUS approach

In (Straub and Papaioannou 2015), based on earlier work published in (Straub 2011), we propose a methodological framework termed BUS, which stands for Bayesian Updating with Structural reliability methods. BUS can be interpreted as an extension of the classical rejection sampling approach to Bayesian analysis. In this approach, samples $\mathbf{x}_k$ are randomly generated from the prior distribution of $\mathbf{X}$. The samples are then accepted with probability $p = cL(\mathbf{x}_k)$. The constant c can be any positive real number that fulfills $c \leq 1/\sup L(\mathbf{x})$. It is straightforward to show that the accepted samples follow the posterior distribution $f_{\mathbf{X}|Z}(\mathbf{x}) \propto f_{\mathbf{X}}(\mathbf{x})L(\mathbf{x})$, e.g. (Smith and Gelfand 1992). The principle of the rejection sampling approach is illustrated in Figure 2a.

The problem with the simple rejection sampling algorithm is its inefficiency. The acceptance probability of samples is equal to $\int_{D_{\mathbf{X}}} cL(\mathbf{x})f_{\mathbf{X}}(\mathbf{x})d\mathbf{x}$, with $D_{\mathbf{X}}$ denoting the domain of definition of $\mathbf{X}$. This probability quickly decreases as the difference between the prior distribution and the likelihood increases, which occurs with increasing amount of data. This is particularly critical if weakly or non-informative priors are used. The central idea of BUS is to deal with this small acceptance probability by employing structural reliability methods that allow to efficiently compute rare event probabilities.
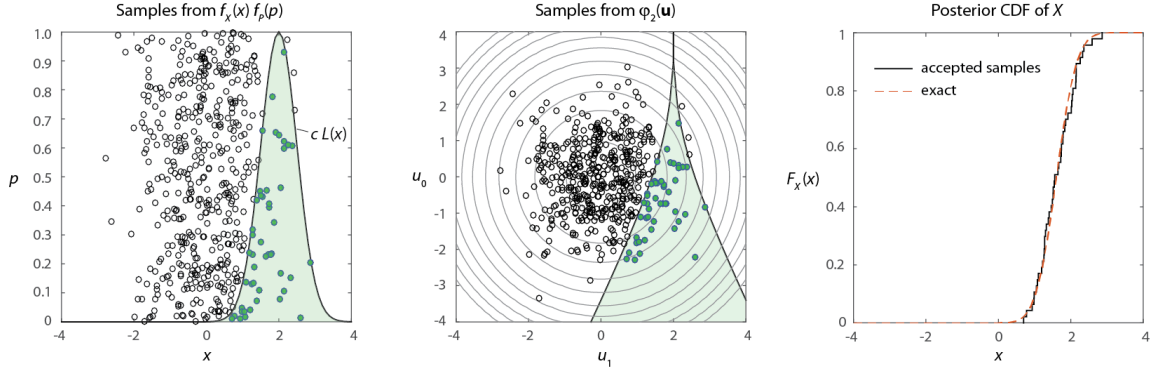
Figure 2. Illustration of the simple rejection sampling algorithm for the case of updating a random variable X, whose prior distribution is the standard normal $f_X(x) \propto exp(-x^2/2)$ and whose likelihood is the normal distribution centered around a measured value 2 with standard deviation $\sigma_m = 0.5$: $L(x) = exp[-1/2 \times (x-2)^2/0.5^2]$. (a) Samples of $f_X(x)f_P(p)$: all samples in the green domain are accepted and follow the posterior distribution; (b) samples from the standard normal distribution, with the acceptance domain according to Eq. (18); (c) empirical CDF corresponding to the accepted samples in (a) and (b), together with the exact posterior CDF.

The rejection sampling principle can be cast in the structural reliability framework by considering the augmented random vector $[P; \mathbf{X}]$, where P is the standard uniform random variable that determines whether a sample is accepted or rejected. In rejection sampling, the posterior distribution of $\mathbf{X}$ is obtained by censoring the joint distribution of P and $\mathbf{X}$ to the domain $\{p \leq cL(\mathbf{x})\}$ and marginalizing $\mathbf{X}$:

$$f_{\mathbf{X}|\mathbf{d}}(\mathbf{x}) \propto \int_0^1 \mathbf{1}_Z(p, \mathbf{x}) \, f_{\mathbf{X}}(\mathbf{x}) \, dp. \tag{12}$$

$\mathbf{1}_Z$ is the indicator function, which takes value one if $\{p \leq cL(\mathbf{x})\}$ and zero otherwise. The proportionality constant in Eq. (12) is $\int_{D_{\mathbf{X}}} \int_0^1 \mathbf{1}_Z(p, \mathbf{x}) \, f_{\mathbf{X}}(\mathbf{x}) \, dp \, dx_1 dx_2 \ldots dx_n$.

We define the observation event as

$$Z = \{P \leq cL(\mathbf{X})\}. \tag{13}$$

Eq. (12) states that the conditional PDF of $\mathbf{X}$ given the data $\mathbf{d}$ is obtained by conditioning the prior distribution on the observation event Z. In contrast to the observation event Z defined according to Eq. (11) (the ABC criterion) this new definition of the observation domain is not an approximation, i.e. it describes the data exactly in a Bayesian framework. Because of this equivalence of Z with the data, it follows that conditioning the probability of F on the data is equivalent to conditioning it on Z:

$$\Pr(F|\mathbf{d}) = \Pr(F|Z). \tag{14}$$

In the remainder, we will write $\Pr(F|Z)$ for the conditional probability of the rare event given the data. It can be obtained by combining Eq. (2) with Eq. (12):

$$
\begin{aligned}
\Pr(F|Z) &= \int_{g(\mathbf{x})\leq 0} f_{\mathbf{X}|\mathbf{d}}(\mathbf{x})\mathrm{d}x_1\mathrm{d}x_2\ldots\mathrm{d}x_n \\
&= \frac{\int_{g(\mathbf{x})\leq 0}\int_0^1 \mathbf{1}_Z(p,\mathbf{x})f_{\mathbf{X}}(\mathbf{x})\,\mathrm{d}p\,\mathrm{d}x_1\mathrm{d}x_2\ldots\mathrm{d}x_n}{\int_{D_{\mathbf{X}}}\int_0^1 \mathbf{1}_Z(p,\mathbf{x})f_{\mathbf{X}}(\mathbf{x})\,\mathrm{d}p\,\mathrm{d}x_1\mathrm{d}x_2\ldots\mathrm{d}x_n}
\end{aligned} \tag{15}
$$

To comply with structural reliability conventions, we define the observation domain $\{p \leq cL(\mathbf{x})\}$ through a limit state function h, such that the domain corresponds to $\{h(p,\mathbf{x}) \leq 0\}$:

$$h(p,\mathbf{x}) = p - cL(\mathbf{x}). \tag{16}$$

Eq. (15) can now be rewritten to

$$
\begin{aligned}
\Pr(F|Z) &= \frac{\int_{g(\mathbf{x})\leq 0 \cap h(p,\mathbf{x})\leq 0} f_{\mathbf{X}}(\mathbf{x})\mathrm{d}p\,\mathrm{d}x_1\mathrm{d}x_2\ldots\mathrm{d}x_n}{\int_{h(p,\mathbf{x})\leq 0} f_{\mathbf{X}}(\mathbf{x})\mathrm{d}p\,\mathrm{d}x_1\mathrm{d}x_2\ldots\mathrm{d}x_n} \\
&= \frac{\Pr[g(\mathbf{X})\leq 0 \cap h(P,\mathbf{X})\leq 0]}{\Pr[h(P,\mathbf{X})\leq 0]}
\end{aligned} \tag{17}
$$

For applying SRM, it is convenient to transform the problem to standard normal space. The corresponding function H is

$$H(\mathbf{u}) = u_0 - \Phi^{-1}\left(cL\left(\mathbf{T}^{-1}(u_1,\ldots,u_n)\right)\right). \tag{18}$$

with Φ^{-1} being the inverse standard normal CDF. U_0 is the standard normal random variable corresponding to P. The observation domain $\{H(\mathbf{u}) \leq 0\}$ corresponding to the simple example of Figure 2a is shown in Figure 2b, together with the transformed samples.

The probability of the rare event F conditional on the data can now be expressed in terms of the standard normal $\mathbf{U}$:

$$\Pr(F|Z) = \frac{\Pr[G(\mathbf{U})\leq 0 \cap H(\mathbf{U})\leq 0]}{\Pr[H(\mathbf{U})\leq 0]} \tag{19}$$

In section 3, we present three SRM for computing the numerator and the denominator of Eq. (19).

2.4.1 Constant c

BUS requires the choice of the constant c. The probabilities in the numerator and denominator of Eqs. (17) and (19) increase linearly with c. If the efficiency of the SRM used for computing these probabilities decreases with decreasing probabilities, then the value of c should be chosen as large as possible, i.e. as close as possible to $[\sup L(\mathbf{x})]^{-1}$. In many applications, this value is not known a-priori. In (Straub and Papaioannou 2015) it is proposed to choose a value of c that is $< [\sup L(\mathbf{x})]^{-1}$ with some probability, which can be achieved by analyzing the likelihood function. In (Betz et al. 2014a) and (Au et al. 2015), it is shown how the constant c can be selected adaptively when applying SuS.

When combined with FORM and FORM-based methods, the performance of the BUS approach can depend on c, but a larger c is not necessarily beneficial in this case. In fact, as we demonstrate in the numerical examples, a smaller value of c can increase the accuracy of line sampling based on FORM.

3 Implementation of BUS for rare events

The application of BUS for updating the probability of a rare event F requires the solution of Eqs. (17) or (19). SRM are applied to efficiently evaluate the numerator and the denominator in these equations. We present the application of three of these methods, FORM, line sampling and SuS, each of which has its specific advantages and disadvantages.

3.1 BUS with FORM

As pointed out earlier, FORM is a powerful method for estimating the probability of rare events in problems with limited number of (relevant) random variables. From all SRM, it is often the one requiring the smallest number of model evaluations. If FORM is used to perform Bayesian updating with BUS following Eq. (19), one has to consider that the shape of the observation domain $\{H(\mathbf{u}) \leq 0\}$ is different from the shapes of the failure domains usually encountered. Consider the observation domain of Figure 2. In Figure 4, the FORM approximation to this domain is illustrated.
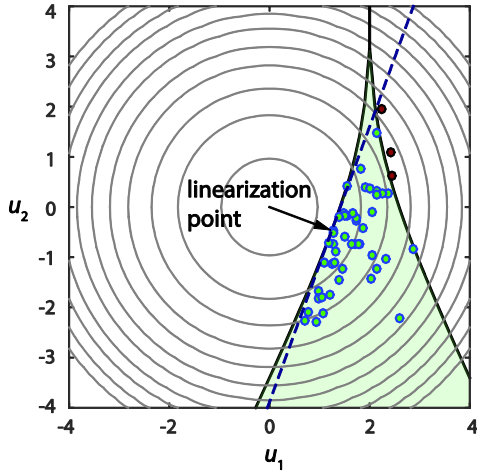
Figure 3. FORM approximation of the observation domain of the example from Figure 2. The dashed line is the linearized surface $\{H(\boldsymbol{u}) = 0\}$. The green dots are the samples from Figure 2 that would be correctly accepted according to the FORM approximation, the red dots are the samples that would be wrongly accepted.

The FORM estimate of the denominator in Eq. (19), $\Pr[H(\mathbf{U}) \leq 0]$, is obtained according to Eqs. (6) and (7), wherein $G(\mathbf{U})$ is replaced with $H(\mathbf{U})$.

The application of FORM in BUS requires the solution of system reliability problems, which are characterized by multiple limit state functions. The numerator in Eq. (19), $\Pr[G(\mathbf{U}) \leq 0 \cap H(\mathbf{U}) \leq 0]$, is an intersection, and the corresponding FORM solution is based on linearizing both functions $G(\mathbf{u})$ and $H(\mathbf{u})$ at the so-called joint design point $\mathbf{u}^*$, identified as follows:

$$\mathbf{u}^* = \arg\min\|\mathbf{u}\|$$
$$\text{s.t. } G(\mathbf{u}) \leq 0, H(\mathbf{u}) = 0 \tag{20}$$

In classical applications of FORM, the second constraint is $H(\mathbf{u}) \leq 0$. Because it can occur that the function H is negative at the origin $\mathbf{0}$, i.e. $H(\mathbf{0}) < 0$, the equality constraint is used instead to ensure that the joint design point is on the boundary of the domain $\{H(\mathbf{u}) \leq 0\}$.

For details on the classical FORM solution to system problems, the reader is referred to (Der Kiureghian 2005). The linear approximations of the two limit state functions are described by their normalized gradient row vectors $\boldsymbol{\alpha}_G^*$ and $\boldsymbol{\alpha}_H^*$, calculated at the joint design point as:

$$\boldsymbol{\alpha}_G^* = -\frac{\nabla G(\mathbf{u}^*)}{\|\nabla G(\mathbf{u}^*)\|} \tag{21}$$

$$\boldsymbol{\alpha}_H^* = -\frac{\nabla H(\mathbf{u}^*)}{\|\nabla H(\mathbf{u}^*)\|} \tag{22}$$

The FORM estimate to the probability $\Pr[G(\mathbf{U}) \leq 0 \cap H(\mathbf{U}) \leq 0]$ is obtained by computing the distance of the linearized surfaces $G(\mathbf{U}) = 0$ and $H(\mathbf{U}) = 0$ from the origin:

$$\beta_i^* = \boldsymbol{\alpha}_i^* \mathbf{u}^* \tag{23}$$

and by determining the correlation coefficient between $G(\mathbf{U})$ and $H(\mathbf{U})$:

$$\rho_{GH}^* = \boldsymbol{\alpha}_G^* \boldsymbol{\alpha}_H^{*\,\mathrm{T}} \tag{24}$$

The FORM estimate is:

$$\Pr[G(\mathbf{U}) \leq 0 \cap H(\mathbf{U}) \leq 0] \approx \Phi_2\left(\begin{bmatrix} -\beta_G^* \\ \beta_H^* \end{bmatrix}; \begin{bmatrix} 1 & -\rho_{GH}^* \\ -\rho_{GH}^* & 1 \end{bmatrix} \right) \tag{25}$$

or

$$\Pr[G(\mathbf{U}) \leq 0 \cap H(\mathbf{U}) \leq 0] \approx \Phi_2\left(-\begin{bmatrix} \beta_G^* \\ \beta_H^* \end{bmatrix}; \begin{bmatrix} 1 & \rho_{GH}^* \\ \rho_{GH}^* & 1 \end{bmatrix} \right) \tag{26}$$

wherein $\Phi_2(\mathbf{B}\,;\mathbf{R})$ is the bivariate standard normal CDF with argument $\mathbf{B}$ and correlation coefficient matrix $\mathbf{R}$. The FORM approximation is illustrated in Figure 4. Equation (25) corresponds to the case where the observation domain is oriented towards the origin, i.e. when $\frac{d}{da} H\big(\boldsymbol{\alpha}_i^* (\beta_i^* + a)\big)$ evaluated at $a = 0$ is positive (Figure 4a). Equation (26) holds if the observation domain is oriented away from the origin, i.e. when $\frac{d}{da} H\big(\boldsymbol{\alpha}_i^* (\beta_i^* + a)\big)$ evaluated at $a = 0$ is negative (Figure 4b)[4].

In some cases, such as the one depicted in Figure 4b, the accuracy of the FORM estimate could potentially be enhanced by considering additional linearization points (see Figure 4c). However, this approach is not recommended in general. In a lower-dimensional setting, the probability contribution of the domain that is mistakenly included is often small, as in the example of Figure 3. In a higher-dimensional setting, the identification of the potentially large number of linearization points is difficult, if not impossible, to achieve. For this reason, in higher dimensions, FORM is not expected to provide accurate estimates for the numerator or the denominator of Eq. (19). However, there are cases in which the errors made in the numerator

---

[4] Note that Eq. (26) is the standard result found in references on FORM system reliability. The result of Eq. (25) is specific to the application of FORM in BUS.

and the denominator are approximately proportional, and FORM can provide good estimates even in high dimensions.
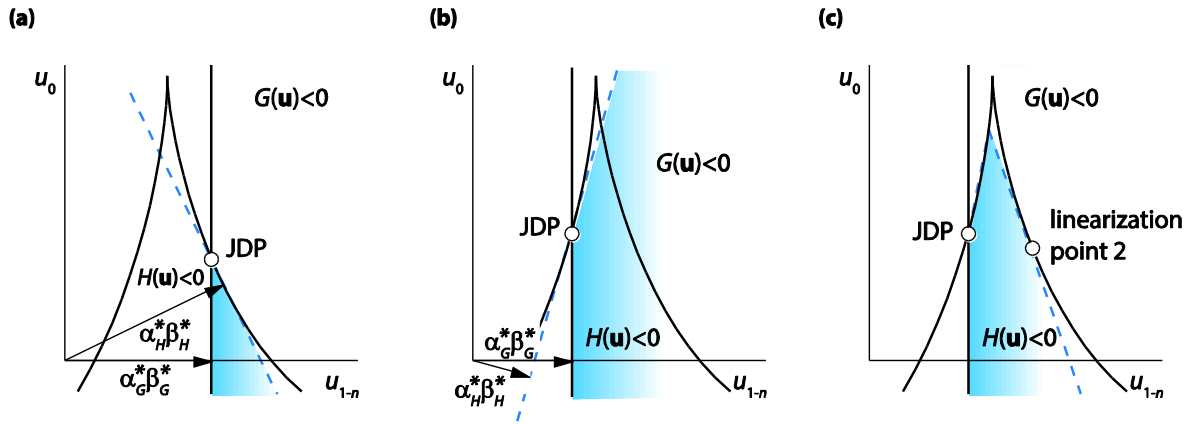
Figure 4. FORM system reliability solution. The blue area is the linearized version of the domain {F ∩ Z}. Case (a): The FORM solution according to Eq. (25) applies. Case (b): The FORM solution according to Eq. (26) applies. (c): as in (b), but with a second linearization point.

When the FORM results are not expected to be accurate, the joint design point following Eq. (20) can nevertheless be used as a basis for dedicated importance sampling methods that can work also in higher dimensions, such as line sampling.

3.2 BUS with Line Sampling

Line sampling (also called axis parallel importance sampling) is an importance sampling technique that is commonly used in structural reliability. The method generates samples at a hyperplane in the standard normal space that is orthogonal to a unit vector $\mathbf{a}$. The vector $\mathbf{a}$ represents an important direction, which is chosen such that it points towards the limit state surface. Line sampling was introduced in (Hohenbichler and Rackwitz 1988) for obtaining a correction factor to FORM estimates of the probability of failure. Therein, the vector $\mathbf{a}$ was taken equal to the unit vector pointing to the design point, i.e. $\mathbf{a} = -\mathbf{u}^*/\|\mathbf{u}^*\|$. The method was further developed in (Koutsourelakis et al. 2004), replacing the initial FORM run with a coarse Monte Carlo simulation to determine a sampling direction that points to the limit state surface.

In the context of BUS, the method is applied to estimate the probability integrals in Eq. (17) in the $(n + 1)$-dimensional standard normal space $\mathbf{U}$. The integration domain in the numerator in Eq. (17) is an intersection of the failure and observation domains. In this case, if a FORM run precedes line sampling, the important direction can be evaluated based on the joint design point defined in Eq. (18). Having determined the important direction $\mathbf{a}$, the sampling space is rotated and reduced by one dimension through the following transformation:

$$\mathbf{V} = \mathbf{RU} \tag{27}$$

wherein $\mathbf{V} = [\mathbf{V}_0; V_n]$, V_n is the coordinate parallel to the vector $\mathbf{a}$, $\mathbf{V}_0$ contains the reduced space that rests on the hyperplane orthogonal to $\mathbf{a}$, and $\mathbf{R}$ is a suitable rotation matrix whose $(n + 1)$th row is the vector $\mathbf{a}$. Because of the rotational symmetry of the standard normal distribution, the vector $\mathbf{V}_0$ follows the n-variate independent standard normal PDF on the hyperplane $v_n = 0$. The method proceeds by generating N independent samples $\{\mathbf{v}_{0k}, k = 1, \dots, N\}$ of $\mathbf{V}_0$. For each sample $\mathbf{v}_{0k}$ a line search is performed to determine the distance $d(\mathbf{v}_{0k})$ from the limit state surface in a direction orthogonal to the hyperplane $v_n = 0$, as illustrated in Figure 5. In cases where the direction intersects two or more boundaries of the integration domain, the distances from each intersection point to the hyperplane need to be computed. The contribution of each sample to the probability integral is set equal to the probability that the standard normal random variable defined on the coordinate v_n at $\mathbf{v}_{0k}$ lies in the integration domain. If the sample intersects the limit state surface only once, then the probability of the sample is evaluated as

$$p_k = \Phi(-d(\mathbf{v}_{0k})) \tag{28}$$

where Φ is the standard normal CDF. For cases where the sample intersects the limit state surface at two points defining the boundaries of the integration domain on the coordinate v_n at $\mathbf{v}_{0k}$, the probability of the sample is obtained as

$$p_k = \Phi\big(-d_l(\mathbf{v}_{0k})\big) - \Phi(-d_u(\mathbf{v}_{0k})) \tag{29}$$

where $d_l(\mathbf{v}_{0k})$ is the distance to the lower boundary and $d_u(\mathbf{v}_{0k})$ is the distance to upper boundary. The probability integral is then estimated as

$$p_{LS} = \frac{1}{N} \sum_{k=1}^{N} p_k \tag{30}$$
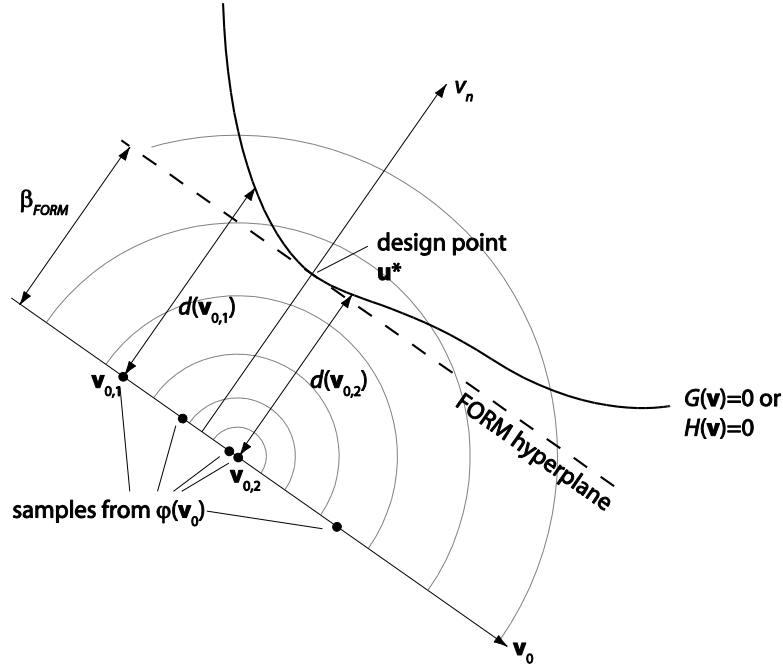
Figure 5. Illustration of the line sampling method.

3.3 BUS with Subset Simulation

Subset simulation, originally developed in (Au and Beck 2001), is an adaptive simulation method that is particularly efficient in estimating rare events in problems with many random variables. The method is based on expressing the probability of a rare event F as a product of larger conditional probabilities, which are estimated with Markov Chain Monte Carlo (MCMC) sampling (Papaioannou et al. 2015). The conditional probabilities are defined in terms of a set of nested intermediate failure events $F_0 \supset F_1 \supset \cdots \supset F_M = F$, where F_0 denotes the certain event. The probability $\Pr(F)$ can be expressed as:

$$\Pr(F) = \Pr\left(\bigcap_{i=1}^{M} F_i\right) = \prod_{i=1}^{M} \Pr(F_i|F_{i-1}) \tag{31}$$

The event F is defined in the standard normal space as $F = \{G(\mathbf{u}) \leq 0\}$. The intermediate events are defined as $F_i = \{G(\mathbf{u}) \leq b_i\}$, where $b_1 > b_2 > \cdots > b_M = 0$. The values of b_i are chosen adaptively such that the estimates of the conditional probabilities correspond to a chosen value p_0, where typically p_0 is chosen as 0.1. This is achieved by simulating N samples of $\mathbf{U}$ conditional on each intermediate failure event F_{i-1}. For each sample, the limit-state function $G(\mathbf{u})$ is evaluated and the samples are ordered in increasing order of magnitude of the limit-state function values. The threshold b_i is set to the p_0-percentile of the ordered samples. The

procedure is repeated until the maximum level M is reached, for which $b_M = 0$. To estimate b_1, unconditional samples of $\mathbf{U}$ are obtained by Monte Carlo sampling. Samples of $\mathbf{U}$ conditional on the events $F_i, i = 1, \dots, M - 1$, are generated by MCMC sampling, using as seeds the samples conditional on F_{i-1} for which $G(\mathbf{u}) \leq b_i$. The sampling procedure conditional on the first intermediate failure domain is illustrated in Figure 6. The probability of the rare event is then estimated as:

$$p_{SuS} = p_0^{M-1} p_M \tag{32}$$

where p_M is the estimate of $\Pr(F_M | F_{M-1})$ and is given by

$$p_M = \frac{1}{N} \sum_{k=1}^{N} \mathbf{1}_F(\mathbf{u}_k^{M-1}) \tag{33}$$

$\mathbf{1}_F$ is the indicator function of the event F and $\{\mathbf{u}_k^{M-1}, k = 1, \dots, N\}$ are samples of $\mathbf{U}$ conditional on F_{M-1}.

BUS requires estimation of the probabilities in the numerator and denominator of Eq. (17). The probability of the observation $\Pr(Z)$ with $Z = \{H(\mathbf{u}) < 0\}$ can be estimated with SuS following the same procedure with intermediate events $Z_0 \supset Z_1 \supset \cdots \supset Z_M$ defined in terms of the observation limit state function $H(\mathbf{u})$. Alternatively, $\Pr(Z)$ can be estimated following the approach proposed in (Betz et al. 2014a) that is based on SuS and additionally estimates the constant c adaptively. To estimate the probability of the intersection of the observation and failure events $\Pr(F \cap Z)$ we define the joint event $F \cap Z$ in terms of the equivalent limit state function $\hat{G}(\mathbf{u}) = \max(G(\mathbf{u}), H(\mathbf{u}))$, where it holds $F \cap Z = \{\hat{G}(\mathbf{U}) \leq 0\}$. Therefore SuS can be applied the same way as for evaluation of the probability of the individual events F or Z, whereby the intermediate events are defined in terms of the limit state function $\hat{G}(\mathbf{u})$.

It is noted that the updated probability $\Pr(F | Z)$ can also be estimated directly following estimation of $\Pr(Z)$ with a new SuS run. This is the procedure we apply in the applications presented later. To this end, we define a set of intermediate events $F_0^* \supset F_1^* \supset \cdots \supset F_M^*$ with $F_i^* = F_i \cap Z$ and $F_0^* = F_0 \cap Z = Z$. The conditional probability can be expressed as

$$\Pr(F | Z) = \frac{\Pr(F \cap Z)}{\Pr(Z)} = \frac{\Pr(\cap_{i=0}^{M} F_i^*)}{\Pr(Z)} = \Pr\left(\bigcap_{i=1}^{M} F_i^* \,\middle|\, F_0^* \right) = \prod_{i=1}^{M} \Pr(F_i^* | F_{i-1}^*) \tag{34}$$

Samples conditional on $F_0^* = Z$ are available from the final step in the estimation of $\Pr(Z)$. The intermediate events $F_i^*, i = 1, \ldots, M-1$ are defined the same way as in standard SuS, and samples conditional on $F_i^*, i = 1, \ldots, M-1$ are obtained by MCMC.

(a) Monte Carlo sampling; identification of intermediate failure domain

(b) Markov chain Monte Carlo sampling at intermediate failure domain
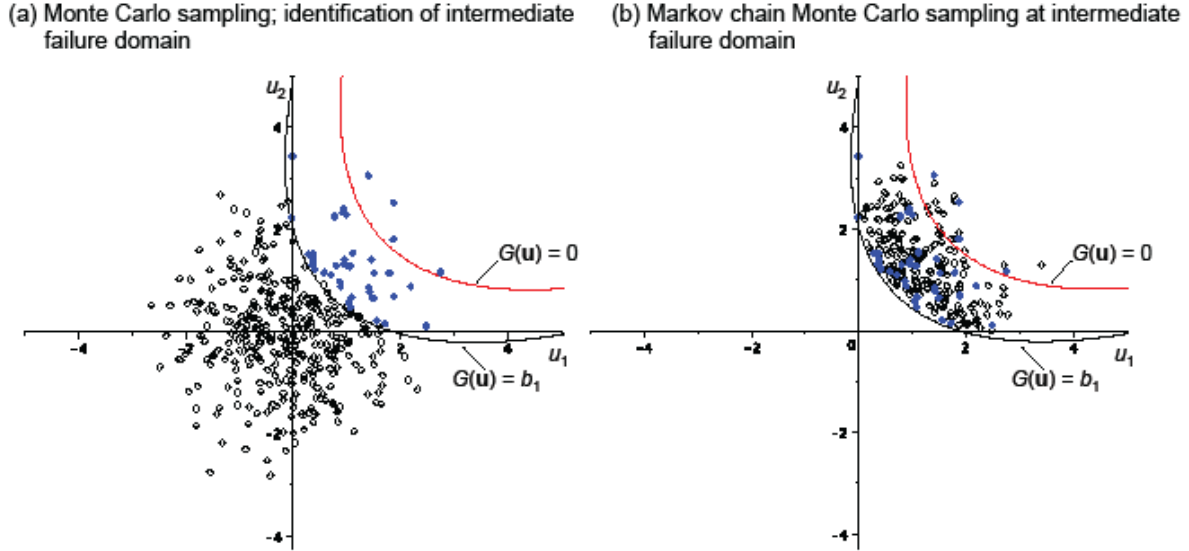
Figure 6. Illustration of the subset simulation method.

4   Applications

4.1   Illustrative example in low dimension

For illustrational purposes, we consider the basic reliability problem: Failure occurs, when the load S exceeds the capacity R: $F = \{R \leq S\}$. The corresponding limit state function defining failure as $F = \{g(\mathbf{X}) \leq 0\}$ is

$$g(\mathbf{X}) = R - S. \tag{35}$$

The load S is Gumbel (extreme value type 1 maxima) distributed with mean 2 and standard deviation 1; the capacity R is lognormal distributed with mean 12 and standard deviation 2. Both random variables are independent, hence only the marginal transformations $u_i = \Phi^{-1}[F_{X_i}(x_i)]$ are necessary for transforming the reliability problem to the standard normal space (U-space) following Eq. (4).

We consider measurements r_m of R that are subject to an additive measurement error. Such measurements can correspond to a quality check of the material after manufacturing. With an

unbiased normal distributed additive measurement error ϵ, the likelihood function describing the measurement r_m is

$$L(r) = \exp\left[-\frac{1}{2}\left(\frac{r - r_m}{\sigma_\epsilon}\right)^2\right] \tag{36}$$

with $\sigma_\epsilon = 1.0$ being the standard deviation of the measurement error. The corresponding limit state function describing this measurement event Z is obtained by inserting this likelihood function into Eq. (16) or (18). The constant c is chosen as 1, corresponding to $1/\sup L(r)$.

We investigate two cases $r_m = 8$ and $r_m = 12$. The resulting limit state functions in U-space are shown in Figure 7. The limit state function for failure G is a function only of U_r and U_s (shown in the upper part of Figure 7), whereas the limit state function describing the observation H is a function of U_r and U_0 (shown in the lower part of Figure 7). The joint design point $\mathbf{u}^*$ is indicated, which is used for the linearization of the limit state functions in the FORM analysis. In case of $r_m = 12$, where the measured value is equal to the prior mean, $\Pr(Z)$ is overestimated by FORM if is linearized solely at its joint design point. This can be avoided by adding a second linearization, as illustrated in Figure 7. However, such a situation will only arise when the probability of the observation is large. Hence in most applications, these probabilities could be calculated with simple MCS.

The results for the two cases are summarized in Table 1. The FORM results are presented together with those from line sampling (LS), subset simulation (SuS), MCS, and the exact solution. For each method, the number of forward model evaluations is provided, to indicate the required computational efforts. We point out that no deep efforts were made to optimize the individual SRM for this application. This applies in particular for FORM, where a standard optimization algorithm was used, and for line sampling, where an improved line search algorithm may potentially lead to a reduced computational effort.

For this trivial problem, it is not surprising that FORM performs well and clearly outperforms the other methods. When comparing the performance of the sampling methods, one has to contrast their accuracy with the number of model calls. The number of samples (and thus the number of model evaluations) can always be reduced at the cost of lower accuracy. Nevertheless, it can be said here that LS, which is based on FORM, is the most exact sampling method among the ones investigated. SuS has a larger variability, and this would still hold if the same number of model evaluations as in IS were carried out. MCS is clearly not ideal, in particular for $r_m = 8$ with a small posterior $\Pr(F|Z)$, because its performance depends directly on the magnitude of $\Pr(F \cap Z)$.
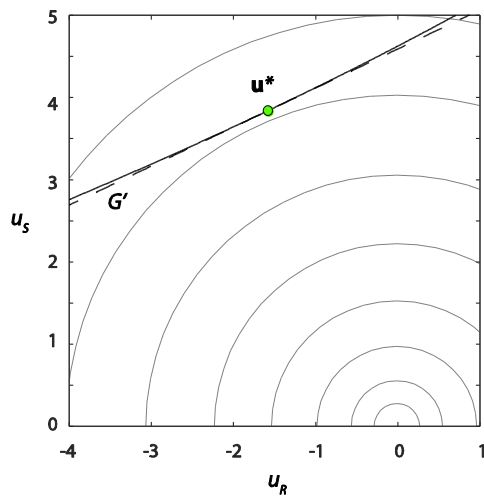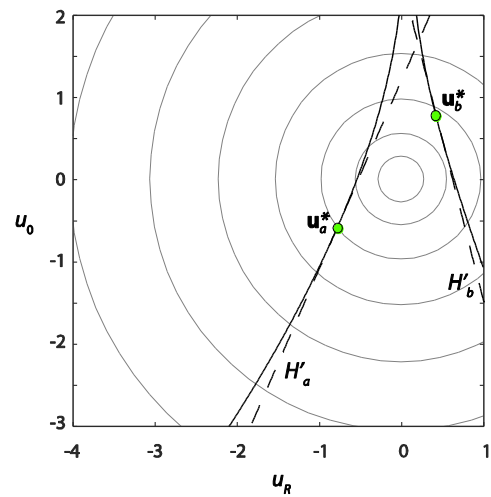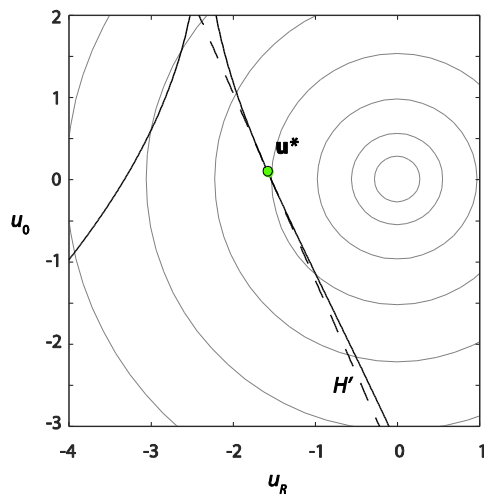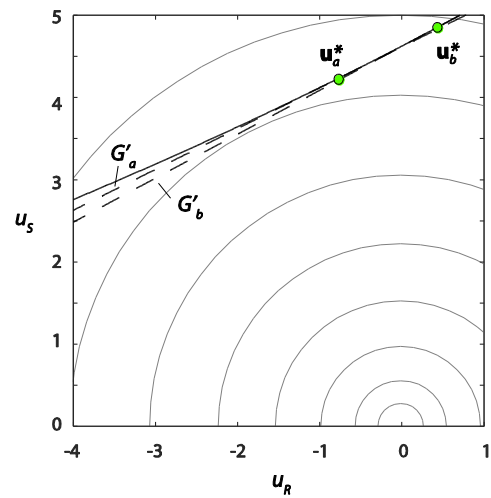
Figure 7. Limit state surfaces of example 1 in standard normal space $G(u) = 0$ and $H(u) = 0$, together with the linear FORM approximations $G'(u) = 0$ and $H'(u) = 0$. Above: failure limit state surface in the $U_R - U_S$ plane; below: observation limit state surface in the $U_R - U_0$ plane. The linearization points are shown as green dots. In case (a), the measurement is away from the prior mean, and a linear approximation at the joint design point is sufficient. In case (b), the measurement is equal to the prior mean, and two linearization points (at the two local minima) give better accuracy.

Table 1. Results of the Bayesian updating. MCS is performed with 10^7 samples, results are shown as 95% confidence interval. SuS is performed with 1000 samples at each subset level. LS is performed with 1000 line searches. Results in square brackets represent the 95% credible interval. The number of model runs are provided for the computation of the denominator $Pr(Z)$ plus the computation of the numerator $Pr(F \cap Z)$.

Case	Method	$Pr(F)$	$Pr(Z)$	$Pr(F \cap Z)$	$Pr(F\|Z)$	# model runs [10^3]
$r_m = 8$	FORM	1.68e-5	8.14e-2	1.06e-5	1.30e-4	0.02+0.07 = 0.09
	SuS	[0.7-3.1]e-5	[6.9-10]e-2	[0.28-2.61]e-5	[0.34-3.11]e-4	2.1+4.2 = 6.3
	LS	[1.61-1.62]e-5	[8.24-8.28]e-2	[0.87-0.98]e-5	[1.06-1.18]e-4	7.6+22.7 = 30.3
	MCS	[1.34-1.84]e-5	[8.24-8.28]e-2	[0.84-1.24]e-5	[1.02-1.50]e-4	10^4
	Exact	1.62e-5	8.26e-2	9.3e-6	1.13e-4	-
$r_m = 12$	FORM	1.68e-5	0.73	1.4e-6	1.9e-6	0.03+0.06 = 0.09
	FORM (sys.)	1.68e-5	0.46	1.4e-6	3.0e-6	0.06+0.06 = 0.12
	SuS	[0.7-3.1]e-5	[0.42-0.48]	[0.3-4.5]e-6	[0.7-10]e-6	1.5+5.5 = 7.0
	LS	[1.61-1.62]e-5	[0.50-0.53]	[1.28-1.52]e-6	[2.6-2.9]e-6	9.8+19.2 = 29.0
	MCS	[1.3-1.8]e-5	0.45	[0.97-2.63]e-6	[2.2-5.8]e-6	10^4
	Exact	1.62e-5	0.45	1.4e-6	3.2e-6	-

4.2 Illustrative example in higher dimensions

To investigate the performance of the algorithms for problems with larger number of input random variables, the first example is extended by formulating the capacity R as a product of R_i's (e.g. component capacities). The limit state function for failure thus reads:

$$g(\mathbf{X}) = \prod_{i=1}^{n_R} R_i - S \tag{37}$$

The R_i's are modelled as lognormal iid random variables, and the distribution parameters of R_i are chosen such that this reliability problem reduces to the one of the first example. We consider two types of measurements.

Firstly, a measurement of the product $R = \prod_{i=1}^{n_R} R_i$ is considered, with the likelihood function of Eq. (36) and $r_m = 8$. This is exactly the same problem as in example 1, hence the dimensionality of the problem could be reduced without any approximation. The MCS and the SuS solutions are not affected by the increased dimensionality, and the results of example 1 still

hold. The interest here is in investigating how the FORM solution is influenced by the (artificial) increase of dimensions, by setting $n_R = 100$. The obtained FORM results are identical to the ones of Example 1, which demonstrates that the method can still work in higher dimensions for problems that could be reduced to lower-dimensional problems. Note that the performance of many existing algorithms for Bayesian analysis are influenced by such an artificial increase of dimensions; e.g. (Betz et al. 2016) show that the performance of the transitional MCMC (TMCMC) proposed in (Ching and Chen 2007) deteriorates strongly under such an artificial increase in dimensions.

Secondly, to investigate a real increase in dimensions, individual measurements of the R_i's are considered. The corresponding likelihood function is

$$L(\mathbf{r}) = \exp\left[-\frac{1}{2}\sum_{i=1}^{n_R}\left(\frac{\ln r_i - \ln r_{m,i}}{\sigma_\epsilon}\right)^2\right] \tag{38}$$

wherein $\sigma_\epsilon = 0.05$ and $r_{m,i} = 8^{1/n_R}$. This likelihood function describes multiplicative lognormal measurement errors. This choice is made because it leads to an analytical solution for the posterior distribution of the R_i's, which facilitates calculating a reference solution.

The analysis is performed for $n_R = 10$ and $n_R = 100$. The results are summarized in Table 2. The FORM results of both the numerator $\Pr(F \cap Z)$ and the denominator $\Pr(Z)$ are off by multiple orders of magnitude. However, the relative error made is approximately the same for both terms, so that the conditional probability is estimated rather accurately. The reason for this is that the shape of $H(\mathbf{u}) = 0$ is similar around the two points utilized for linearizing $H(\mathbf{u})$ in the computations of $\Pr(F \cap Z)$ and $\Pr(Z)$, and $G(\mathbf{u})$ is only weakly non-linear. This behavior can be found in quite many problems, however, it is typically difficult to know whether or not it holds in a particular case. Therefore, a line sampling analysis should ideally be added to the FORM.

Line sampling provides accurate results for $n_R = 10$, but less so for $n_R = 100$, if the constant $c = 1$ is used. However, the LS results strongly improve if $c = 10^{-2}$ is used, as evident from Table 2. With this modified value of c, a very good accuracy is achieved for all investigated n_R. This is explained with the change of the shape of the limit state surface as c is descreased. The accuracy remains good for any other investigated value of $c < 10^{-1}$. It is noted that the FORM results also changes with c, but this change is only minor, in the order of 10% of the final result.

Finally, the performance of MCS and SuS is not affected by the increase of dimensions. Overall, FORM in combination with line sampling seems to be a good choice for this problem, but SuS leads to a comparable trade-off between accuracy and number of model evaluations, with the advantage of being more robust (unlike for LS, the optimal value of c is known).

Table 2. Results of the Bayesian updating. MCS is performed with 10^7 samples. SuS is performed with 1000 samples at each subset level. LS with 1000 line searches. Results in square brackets represent the 95% credible interval. The number of model runs are provided for the computation of the denominator $Pr(Z)$ plus the computation of the numerator $Pr(F \cap Z)$.

Case	Method	$Pr(F)$	$Pr(Z)$	$Pr(F \cap Z)$	$Pr(F\|Z)$	# model runs [10^3]
$n_R = 10$	FORM	1.68e-5	0.15	1.22e-5	8.0e-5	0.06+0.11 = 0.17
	SuS	[0.7-3.1]e-5	[4.3-7.5]e-3	[0.3-21]e-7	[2.1-35]e-5	3.2+4.5 = 7.7
	LS ($c = 1$)	[1.61-1.62]e-5	[4.7-6.7]e-3	[1.9-6.4]e-7	[3.1-12]e-5	14+18= 32
	LS ($c = 10^{-2}$)	[1.61-1.62]e-5	[5.0-6.4]e-5	[2.9-5.1]e-9	[5.0-9.2]e-5	6.3+13.9 = 20.2
	MCS	[1.4-1.9]e-5	[5.7-5.8]e-3	[0-6.7]e-7	[0-11.5]e-5	10^4
	Exact	1.62e-5			6.8e-5	
$n_R = 100$	FORM	1.68e-5	0.71	1.65e-5	2.33e-5	0.5+1.9 = 2.4
	SuS	[0.7-3.1]e-5	[3.2-5.5]e-3	[0.07-5.1]e-7	[0.2-12]e-5	3.4+5.0= 8.4
	LS ($c = 1$)	[1.61-1.62]e-5	[3.1-5.5]e-3	[0-1.1]e-6	[0-25]e-5	7.0+10.0= 17.0
	LS ($c = 10^{-2}$)	[1.61-1.62]e-5	[4.0-4.4]e-5	[0.7-1.1]e-9	[1.6-2.6]e-5	5.0+13.8=18.8
	MCS	[1.4-1.9]e-5	[4.2-4.3]e-3	[0.025-3.7]e-7	[0.06-8.6]e-5	10^4
	Exact	1.62e-5			2.1e-5	

4.3 Diffusion problem

We consider a 1D steady state diffusion problem. It is described by the following diffusion equation on the unit interval $D = [0,1]$:

$$\frac{d}{dx}\left(a(x)\frac{du}{dx}\right) + b(x) = 0 \tag{39}$$

with random diffusivity $a(x)$.

We distinguish two situations: (a) is related to the measurements, and (b) is related to the potential rare event of interest. In situation (a), the diffusivity $a(x)$ is inferred from measurements of the field $u(x)$ at a specified number of locations, performed during a controlled experiment. This inverse problem could be considered a prototype of the estimation of the hydraulic conductivity of an aquifer from pumping tests. The source term that models the applied pumping rate is given as:

$$b(x) = \sum_{i=1}^{N} \frac{s_i}{\sqrt{2\pi}\sigma_i} \exp\left(-\frac{(l_i - x)^2}{2\sigma_i^2}\right) \tag{40}$$

The above involves N localized sources (pumped wells), each centered at location l_i, with strength s_i and width σ_i. The boundary conditions are set to zero ($u(0) = u(1) = 0$) at both boundaries. This prototype inverse problem is the steady state version of the inverse problem investigated in (Marzouk and Najm 2009). We consider three sources at locations $l_1 = 0.25$, $l_2 = 0.5$ and $l_3 = 0.75$ with identical strengths $s_i = 10$ and widths $\sigma_i^2 = 10^{-3}$. The sensors that measure the field u are uniformly spaced on D, excluding the endpoints. We use $m = 11$ sensors.

In situation (b), the domain D is subjected to a flow from left to right. That is, the source term is zero ($b(x) = 0$) and the boundary conditions are set to inflow at the left boundary ($u(0) = 1$) and outflow at the right boundary ($u(1) = 0$). The flow rate is evaluated through

$$q(x) = -a(x)\frac{du}{dx} \tag{41}$$

The diffusion equation is solved with linear finite elements on a uniform grid with spacing $h = 1/48$. The event of interest is defined as the flow rate at the right boundary $q(1)$ exceeding a prescribed threshold $q_t = 1.3$. The corresponding limit state function is $g(a) = q_t - q(1)$.

We model the prior of the log-diffusivity $\ln a(x)$ with a Gaussian random field with mean $\mu_{\ln a} = 0.1$, standard deviation $\sigma_{\ln a} = 0.2$ and autocorrelation coefficient function $\rho_{\ln a}(\Delta x) = \exp(-\Delta x / \lambda)$ with $\lambda = 0.3$. To represent the random field $\ln a(x)$, we apply its Karhunen–Loève expansion (Ghanem and Spanos 1991) which takes the following form

$$\ln a(x) = \mu_{\ln a} + \sigma_{\ln a} \sum_{i=1}^{n} \sqrt{\theta_i} \chi_i(x) U_i \tag{42}$$

where $\{\theta_i, \chi_i\}$ are the eigenpairs of $\rho_{\ln a}$, which are know analytically for the applied exponential correlation model (Ghanem and Spanos 1991), and $U_i, i = 1, \ldots, n$, are independent

standard normal random variables. The expansion is truncated after 10 terms, i.e. $n = 10$. We employ this discrete representation of the log-diffusivity and hence learn the random variables $U_i, i = 1, \dots, n$, in situation (a). The same random variables are used to define the failure event in situation (b).

To construct the measurements in (a), we employ a target profile that is randomly sampled from the prior distribution of $\ln a(x)$, through drawing a sample from the prior distribution of the U_i's. Using the generated target profile, we solve the forward model to evaluate the values of u at the sensor locations and apply an additive Gaussian noise with standard deviation $\sigma_\epsilon = 0.1$ to simulate measured values $u_{m,i}$. The corresponding likelihood function reads:

$$L(a) = \exp\left[-\frac{1}{2} \sum_{i=1}^{m} \left(\frac{u_i(a) - u_{m,i}}{\sigma_\epsilon} \right)^2 \right] \tag{43}$$

where the $u_i(a)$ denote the solution of the diffusion equation for a realization of the diffusivity a at the sensor locations. The limit state function that describes the measurement event, denoted Z, is obtained by substituting the likelihood function in Eq. (16). It is noted that the random variables in the Karhunen–Loève expansion are already standard normal; therefore there is no need for a transformation of the random variable space. The constant c is selected such that it holds $c < [\sup L(a)]^{-1}$ with a probability 0.05 (see Annex A in Straub and Papaioannou 2015). When using BUS with SuS to estimate $\Pr(Z)$, samples of the posterior distribution are obtained as a by-product of the reliability evaluation. The posterior statistics of the log-diffusivity are summarized in Figure 8. Therein, the posterior median and 95% credible interval obtained from the posterior samples are depicted. It is shown that the Bayesian inversion identifies accurately true profile of the log-diffusivity.
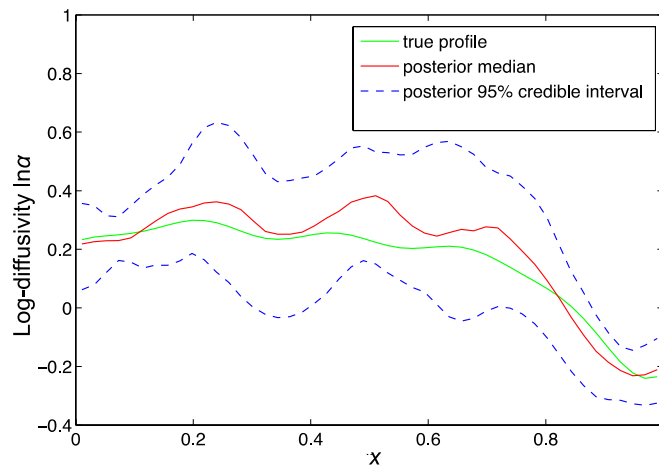
Figure 8. Posterior median and 95% credible interval of the log-diffusivity profile computed with BUS and SuS with 1000 samples per level.

The results of the reliability analysis in situation (b) are shown in Table 3. Comparing the credible bounds of the LS and SuS, it is shown that LS exhibits much smaller bounds than SuS. The bounds of SuS for the posterior probability are notably large. This is because the shape of the observation domain becomes narrow when a large number of measurements is included, which influences the performance of the MCMC algorithm within SuS. In particular, the shape of the observation region favors clustering of the MCMC samples around the seeds of the chains at advanced subset levels. LS performs significantly better, although the variability of the simulation outcomes for $\Pr(F \cap Z)$ is still considerably high, which is attributed to the small size of the intersection of the observation and failure domains. The mean estimate of LS for $\Pr(F)$ is 6.7e-2, for $\Pr(Z)$ 3.65e-6, for $\Pr(F \cap Z)$ 4.35e-9 and for $\Pr(F|Z)$ 1.24e-3. Comparing these values with the FORM results, we see that although the FORM estimates for $\Pr(Z)$ and $\Pr(F)$ differ considerably, the difference is much smaller for $\Pr(F|Z)$. This is because the relative errors for $\Pr(Z)$ and $\Pr(F \cap Z)$ are approximately the same, and hence cancel out in the estimation of $\Pr(F|Z)$. The FORM estimate of the prior probability $\Pr(F)$ is slightly larger compared to the mean LS estimate which indicates that the failure surface is nonlinear around the design point and suggests a convex shape of the failure region.

Table 3. Results of the Bayesian updating. SuS is performed with 1000 samples at each subset level. LS is performed with 1000 line searches. Results in square brackets represent the 95% credible interval from repeated simulation runs. The number of model runs are provided for the computation of the denominator $\Pr(Z)$ plus the computation of the numerator $\Pr(F \cap Z)$.

Method	$\Pr(F)$	$\Pr(Z)$	$\Pr(F \cap Z)$	$\Pr(F|Z)$	# model runs [10^3]
FORM	8.01e-2	2.9e-4	1.6e-7	5.6e-4	0.15+0.17=0.32
SuS	[5.4-8.5]e-2	[0.3-17.0]e-6	[0.0011-26.0]e-9	[0.0069-58.2]e-4	5.6+4=9.6
LS	[6.64-6.75]e-2	[2.2-5.5]e-6	[1.4-9.3]e-9	[4.0-26.5]e-4	9.4+10=19.4

4.4 Foundation stability

As final example, we consider a problem from geotechnical engineering, related to the stability of a foundation. The foundation has a width of 1.5m; after construction it is loaded eccentrically with load P, where the lever arm is 0.5m and P follows a Gumbel distribution with mean 1MN and 10% coefficient of variation. At an intermediate construction stage a centric load F of 0.4MN is applied; the displacements at the left and right ending of the foundation are measured as $\hat{x}_l = 1\text{cm}$ and $\hat{x}_r = 1.5\text{cm}$, see Figure 9.

The additive measurement/modelling error is assumed to follow a normal distribution with zero mean and a standard deviation of $\sigma_\varepsilon = 0.5\text{cm}$; the two errors are correlated with a correlation coefficient of $\rho = 0.9$ (thus, it is implicitly assumed that modelling errors are dominating compared to measurement errors).

Serviceability of the foundation is ensured if the inclination of the foundation under the final loading P is smaller than 4 degrees; i.e. the failure event corresponds to this angle being exceeded: $g(\mathbf{x}) = 4° - \alpha(\mathbf{x})$.
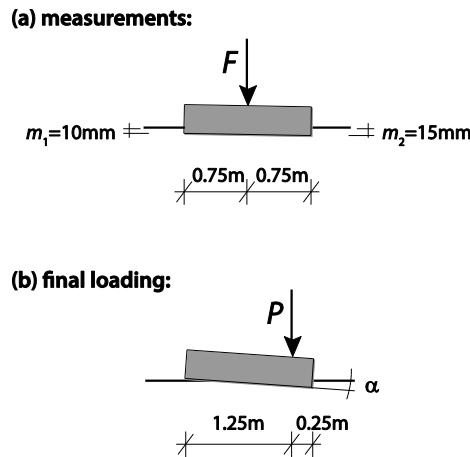
Figure 9. Loading of the foundation (a) during the measurements and (b) in the final state.

The soil is modelled as linear elastic, with a Young's modulus E that is a spatial random field and a fixed Poisson ratio of 0.35. E is modeled as Log-Normal random field with a mean of 40MPa and a coefficient of variation of 50%. The correlation coefficient function between points $\mathbf{x}$ and $\mathbf{x}'$ of the underlying Gaussian random field is $\rho_{\mathbf{x},\mathbf{x}'} = \exp(-\Delta x/l_x - \Delta y/l_y)$, where Δx, Δy is the horizontal distance between points $\mathbf{x}$ and $\mathbf{x}'$, respectively, and $l_x = 20\text{m}$, $l_y = 5\text{m}$ are the correlation lengths in horizontal and vertical directions. The depth of the soil layer is 8m, followed by a sandstone layer whose influence on the analysis is negligible. On each side of the foundation, a soil-stripe of 15m is modeled explicitly. The mechanical model as well as the random field model is discretized and solved by means of higher-order finite elements (Szabó et al. 2004). The finite element mesh is depicted in Figure 10. A finite-element discretization of the Karhunen-Loeve expansion with 100 terms is used to represent the random field (Betz et al. 2014b). The order of the shape functions of the mechanical model is 4, the order of the shape functions used to represent the random field is 8.

The results of the analysis are listed in Table 4. The FORM results match well with the results of the other investigated methods. To enable a direct comparison of LS with SuS, the former is

run additionally with 160 line samples, which results in approximately the same number of model evaluations as required for SuS. This comparison show that the performance of LS is superior to SuS in this example.
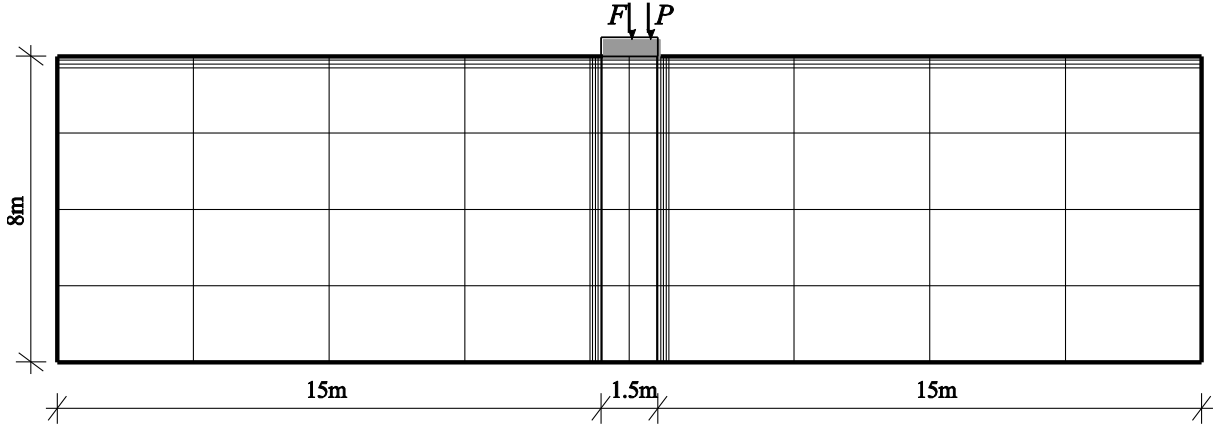
Figure 10. Finite element mesh used to discretize the soil: the order of the shape functions of the mechanical model is 4, the order of the shape functions used to represent the random field is 8.

Table 4. Results of the Bayesian updating. MCS is performed once with approximately 10^6 samples, results are shown as 95% credible interval. SuS is repeatedly performed with 1000 samples at each subset level, results are shown as 95% credible interval. LS is performed repeatedly with either 1000 or 160 line searches each run. The number of model runs are provided for the computation of the denominator $Pr(Z)$ plus the computation of the numerator $Pr(F \cap Z)$.

Method	$Pr(F)$	$Pr(Z)$	$Pr(F \cap Z)$	$Pr(F|Z)$	# model runs [10^3]
FORM	1.4e-2	9.9e-2	2.8e-5	2.8e-4	1.5+1.1 = 2.6
SuS	[1.2-2.1]e-2	[5.4-8.1]e-2	[0.6-5.5]e-5	[0.9-8.5]e-4	2.2+3.7 = 5.9
LS (1000)	[1.55-1.58]e-2	[6.4-6.8]e-2	[1.7-2.4]e-5	[2.7-3.5]e-4	7.1+30.1 = 37.2
LS (160)	[1.54-1.60]e-2	[6.1-7.1]e-2	[1.4-3.0]e-5	[2.2-4.4]e-4	0.9+4.8 = 5.7
MCS	[1.5-1.6]e-2	[6.5-6.6]e-2	[1.1-2.7]e-5	[1.7-4.1]e-4	1000

5 Concluding remarks

The BUS approach presented in this paper establishes an analogy between Bayesian analysis and rare event probability estimation. Thereby, the likelihood function describing the data is transformed into an equivalent (rare) event Z. In doing so, the BUS approach enables methods

developed for estimating rare event probabilities to be applied to Bayesian analysis, with some modifications. As we show in this paper, this is effective when performing Bayesian updating of rare event probabilities. Such applications are of (growing) relevance in the assessment of technological and anthropogenic systems, where monitoring strategies are increasingly used to ensure sufficient reliability, but is relevant also in many other fields of engineering and science. As we show, the equivalent observation event Z of the BUS approach has some similarities to the rejection criterion used in ABC. However, unlike the latter, BUS does not require to solve an approximate problem.

The computational efficiency of the BUS framework is a function of the structural reliability methods (SRM) used to compute the rare event probabilities $\Pr(Z)$ and $\Pr(F \cap Z)$. In this paper we have demonstrated and investigated three SRM: FORM, line sampling (LS) and subset simulation (SuS). Their efficiency, as expressed by the number of model evaluations and the 95% credible interval of the resulting posterior failure probability, has been assessed through a set of numerical examples. However, it is not the goal of this paper to make ultimate statements about the efficiency of the individual SRM. The methods used here can potentially be further optimized to give the same accuracy with fewer model evaluations (in particular LS). Nevertheless, the efficiencies reported are in the same order of magnitude as could be achieved with optimized algorithms and thus do allow one to draw some conclusions.

The performance of the three investigated SRM vary among the investigated examples. Surprisingly, the FORM result for the posterior failure probability $\Pr(F|Z)$ is fairly accurate in all investigated cases, because the relative errors made in the approximations of $\Pr(Z)$ and $\Pr(F \cap Z)$ are similar. While the latter terms individually are overestimated by a factor of up to 100, the relative error in estimating $\Pr(F|Z)$ is in the order of 0.1 to 0.2 for most examples, and in the order of 1 in the worst case (the diffusion example). However, it is clear that one should not rely on FORM results alone without having a good understanding of the shape of the linearized domains, which is difficult to achieve in higher dimensions. For this reason, FORM results should be verified with an alternative method. LS based on the FORM design point is an option in these cases. In the numerical investigations presented here (and in others not presented), LS has consistently given accurate results, as long as the value of the constant c, necessary for defining the observation event Z, is chosen sufficiently small. However, LS will not perform as good if the FORM algorithm does not find the correct design point.

The optimization problem of finding the FORM design point cannot always be solved, in particular when the number of random variables is large. In these cases, BUS can only be implemented with SRM that do not rely on the design point. In this paper, we have considered

SuS as an effective method of this class. In some of the numerical applications, its efficiency was comparable to LS, in some it was lower. Nevertheless, its accuracy is acceptable for many applications, and it can be improved simply by increasing the number of samples.

The strength of the BUS approach is that it leaves open the possibility for applying many of the other SRM. In particular, alternative importance sampling techniques available for analyzing rare events may outperform the methods presented here in certain applications. It is left to future research to investigate these. However, in many instances, the choice of a particular method is as much guided by the preferences of the analyst than by some objective efficiency criteria. We believe that one should be pragmatic in this regard and use "whatever works", as long as the necessary accuracy can be achieved.

We have not included a direct comparison of BUS with existing methods for Bayesian analysis of rare events, which are based on first approximating the posterior PDF and then solving the reliability problem. Our results indicate that BUS can be more efficient, but to provide a fair comparison is difficult. On the one hand, the efficiency of the BUS approach is a function of the SRM method used, and the optimal SRM is problem-dependent and only a subset of them has been considered here. On the other hand, the efficiency of alternative methods depend strongly on their specific implementation.

In our view, the main advantage of BUS over existing methods is the flexibility it provides by drawing upon a large set of SRM, which can be selected problem specific. In contrast to existing approaches, the BUS approach allows to work entirely in standard normal space, which enables or simplifies the use of many SRM, including SuS. In this context it is interesting to note that also TMCMC, which is used to generate samples from the posterior PDF in the alternative approach presented by (Jensen et al. 2013, Hadjidoukas et al. 2015), can potentially be improved by working in standard normal space, as we show in (Betz et al. 2016).

The application examples investigated in this paper are simplified yet representative of real applications, which demonstrate that the method as-is can be used for actual problems in practice. In problems where FORM and related methods are suitable for computing the unconditional $\Pr(F)$, the BUS method in conjunction with the presented SRM will likely be suitable for computing the conditional $\Pr(F|Z)$. As discussed in (Rackwitz 2001), the performance of FORM is surprisingly good for many non-linear problems in lower dimensions, and line sampling can correct errors in higher dimensions. However, it is clear that for highly non-linear system behavior, the methods as implemented in this paper may not perform well, and one should carefully analyze the results in these cases.

Finally, when model input uncertainties are described by non-informative prior distributions, the BUS approach is not effective. However, in most real physical systems, one does have prior information on the input parameters. If one does not, it is still possible to use some of the data to determine a prior distribution through an alternative method, and then include the rest of the data through BUS. In analogy to the use of non-informative priors, the BUS approach will have difficulties when the likelihood function is highly peaked relative to the prior distribution. When this leads to a posterior distribution that lies on a lower-dimensional manifold, the SRM described in this paper to be used within BUS will not be effective or might fail entirely. It remains to be investigated if other methods can be used within the BUS approach in such cases.

In conclusion, the BUS approach enables the use of existing methods for rare event probability estimation for Bayesian analysis. As we demonstrate through numerical examples, the approach works well for a variety of practically relevant situations. Nevertheless, there is significant potential for further developing and enhancing methods for estimating the rare event probabilities within BUS.

Acknowledgments

References

Allaix, D. and V. Carbone (2015). An efficient coupling of FORM and Karhunen–Loève series expansion. *Engineering with Computers*: 1-13.

Au, S.-K. and J. L. Beck (2001). Estimation of small failure probabilities in high dimensions by subset simulation. *Probabilistic Engineering Mechanics* **16**(4): 263-277.

Au, S. and J. L. Beck (1999). A new adaptive importance sampling scheme for reliability calculations. *Structural Safety* **21**(2): 135-158.

Au, S. K., F. A. DiazDelaO and I. Yoshida (2015). Bayesian Updating and Model Class Selection with Subset Simulation. eprint arXiv:1510.06989.

Beaumont, M. A., J.-M. Cornuet, J.-M. Marin and C. P. Robert (2009). Adaptive approximate Bayesian computation. *Biometrika*: asp052.

Beck, J. and L. Katafygiotis (1998). Updating Models and Their Uncertainties. I: Bayesian Statistical Framework. *Journal of Engineering Mechanics* **124**(4): 455-461.

Beck, J. L. (2010). Bayesian system identification based on probability logic. *Structural Control and Health Monitoring* **17**(7): 825-847.

Bedford, T. and R. Cooke (2001). *Probabilistic risk analysis: foundations and methods*, Cambridge University Press.

Betz, W., I. Papaioannou and D. Straub (2014a). Adaptive variant of the BUS approach to Bayesian updating *Eurodyn 2014*. Porto, Portugal.

Betz, W., I. Papaioannou and D. Straub (2014b). Numerical methods for the discretization of random fields by means of the Karhunen–Loève expansion. *Computer Methods in Applied Mechanics and Engineering* **271**(0): 109-129.

Betz, W., I. Papaioannou and D. Straub (2016). Translational Markov Chain Monte Carlo: Observations and Improvements. *Journal of Engineering Mechanics* in print.

Botev, Z. I., D. P. Kroese and T. Taimre (2007). Generalized cross-entropy methods with applications to rare-event simulation and optimization. *Simulation* **83**(11): 785-806.

Bourinet, J. M., F. Deheeger and M. Lemaire (2011). Assessing small failure probabilities by combined subset simulation and Support Vector Machines. *Structural Safety* **33**(6): 343-353.

Breitung, K. (1984). Asymptotic approximations for multinormal integrals. *Journal of Engineering Mechanics* **110**(3): 357-366.

Bucher, C. and U. Bourgund (1990). A fast and efficient response surface approach for structural reliability problems. *Structural safety* **7**(1): 57-66.

Bucher, C. G. (1988). Adaptive sampling — an iterative fast Monte Carlo procedure. *Structural Safety* **5**(2): 119-126.

Cérou, F., P. Del Moral, T. Furon and A. Guyader (2012). Sequential Monte Carlo for rare event estimation. *Statistics and Computing* **22**(3): 795-808.

Chiachio, M., J. L. Beck, J. Chiachio and G. Rus (2014). Approximate Bayesian Computation by Subset Simulation. *SIAM Journal on Scientific Computing* **36**(3): A1339-A1358.

Ching, J. and Y. Chen (2007). Transitional Markov Chain Monte Carlo Method for Bayesian Model Updating, Model Class Selection, and Model Averaging. *Journal of Engineering Mechanics* **133**(7): 816-832.

Cornell, C. A. (1968). Engineering seismic risk analysis. *Bulletin of the Seismological Society of America* **58**(5): 1583-1606.

Csilléry, K., M. G. Blum, O. E. Gaggiotti and O. François (2010). Approximate Bayesian computation (ABC) in practice. *Trends in ecology & evolution* **25**(7): 410-418.

Del Moral, P., A. Doucet and A. Jasra (2006). Sequential Monte Carlo samplers. *Journal of the Royal Statistical Society: Series B* **68**(3): 411-436.

Der Kiureghian, A. (2005). First- and second-order reliability methods. *Engineering design reliability handbook*. E. Nikolaidis, D. M. Ghiocel and S. Singhal. Boca Raton, FL., CRC Press.

Der Kiureghian, A. and P.-L. Liu (1986). Structural reliability under incomplete probability information. *Journal of Engineering Mechanics* **112**(1): 85-104.

Dessai, S. and M. Hulme (2004). Does climate adaptation policy need probabilities? *Climate policy* **4**(2): 107-128.

Ditlevsen, O. and H. O. Madsen (1996). *Structural reliability methods*. Chichester [u.a.], Wiley.

Duenas-Osorio, L. and S. M. Vemuru (2009). Cascading failures in complex infrastructure systems. *Structural safety* **31**(2): 157-167.

Elsheikh, A. H., M. F. Wheeler and I. Hoteit (2014). Hybrid nested sampling algorithm for Bayesian model selection applied to inverse subsurface flow problems. *Journal of Computational Physics* **258**(0): 319-337.

Engelund, S. and R. Rackwitz (1993). A benchmark study on importance sampling techniques in structural reliability. *Structural safety* **12**(4): 255-276.

Fearnhead, P. and D. Prangle (2012). Constructing summary statistics for approximate Bayesian computation: semi‐automatic approximate Bayesian computation. *Journal of the Royal Statistical Society: Series B (Statistical Methodology)* **74**(3): 419-474.

Gelman, A. (2004). *Bayesian data analysis*. Boca Raton, Fla., Chapman & Hall/CRC.

Ghanem, R. G. and P. D. Spanos (1991). *Stochastic Finite Elements: A Spectral Approach*. New York, Springer.

Hadjidoukas, P. E., P. Angelikopoulos, C. Papadimitriou and P. Koumoutsakos (2015). Π4U: A high performance computing framework for Bayesian uncertainty quantification of complex models. *Journal of Computational Physics* **284**(0): 1-21.

Hohenbichler, M. and R. Rackwitz (1981). Non-Normal Dependent Vectors in Structural Safety. *Journal of the Engineering Mechanics Division-Asce* **107**(6): 1227-1238.

Hohenbichler, M. and R. Rackwitz (1988). Improvement of second-order reliability estimates by importance sampling. *Journal of Engineering Mechanics* **114**(12): 2195-2199.

Jensen, H., C. Vergara, C. Papadimitriou and E. Millas (2013). The use of updated robust reliability measures in stochastic dynamical systems. *Computer Methods in Applied Mechanics and Engineering* **267**: 293-317.

Katafygiotis, L. S. and K. M. Zuev (2007). Geometric insight into the challenges in solving high dimensional reliability problems. *Probabilistic Engineering Mechanics* **23**: 208-218.

Kavetski, D., G. Kuczera and S. W. Franks (2006). Bayesian analysis of input uncertainty in hydrological modeling: 1. Theory. *Water Resources Research* **42**(3): n/a-n/a.

Koutsourelakis, P., H. Pradlwarter and G. Schuëller (2004). Reliability of structures in high dimensions, part I: algorithms and applications. *Probabilistic Engineering Mechanics* **19**(4): 409-417.

Kurtz, N. and J. Song (2013). Cross-entropy-based adaptive importance sampling using Gaussian mixture. *Structural Safety* **42**: 35-44.

Li, J., J. Li and D. Xiu (2011). An efficient surrogate-based method for computing rare failure probability. *Journal of Computational Physics* **230**(24): 8683-8697.

Li, J. and D. Xiu (2010). Evaluation of failure probability via surrogate models. *Journal of Computational Physics* **229**(23): 8966-8980.

Liu, P.-L. and A. Der Kiureghian (1991). Optimization algorithms for structural reliability. *Structural Safety* **9**: 161-177.

Madsen, H. O. (1987). Model updating in reliability theory. *ICASP 5, Int. Conf. on Appl. of Statistics and Prob. in Soil and Struct.* Vancouver**:** 565-577.

Madsen, H. O., S. Krenk and N. C. Lind (1985). *Methods of structural safety*. Englewood Cliffs, NJ, Prentice-Hall.

Marin, J.-M., P. Pudlo, C. P. Robert and R. J. Ryder (2012). Approximate Bayesian computational methods. *Statistics and Computing* **22**(6): 1167-1180.

Marzouk, Y. M. and H. N. Najm (2009). Dimensionality reduction and polynomial chaos acceleration of Bayesian inference in inverse problems. *Journal of Computational Physics* **228**(6): 1862-1902.

Melchers, R. E. (1999). *Structural reliability analysis and prediction*, John Wiley.

Paffrath, M. and U. Wever (2007). Adapted polynomial chaos expansion for failure detection. *Journal of Computational Physics* **226**(1): 263-281.

Papadimitriou, C., J. L. Beck and L. S. Katafygiotis (2001). Updating robust reliability using structural test data. *Probabilistic Engineering Mechanics* **16**(2): 103-113.

Papaioannou, I., W. Betz, K. Zwirglmaier and D. Straub (2015). MCMC algorithms for subset simulation. *Probabilistic Engineering Mechanics* **41**: 89-103.

Papaioannou, I., C. Papadimitriou and D. Straub (2014). Sequential Importance Sampling for Structural Reliability. *17th IFIP WG 7.5 Conference on Reliability and Optimization of Structural Systems*. Wuangshan, China.

Paté-Cornell, M. E. (1994). Quantitative safety goals for risk management of industrial facilities. *Structural Safety* **13**(3): 145-157.

Peck, R. B. (1969). Advantages and limitations of the observational method in applied soil mechanics. *Geotechnique* **19**(2): 171-187.

Pradlwarter, H. J., G. I. Schuëller, P. S. Koutsourelakis and D. C. Charmpis (2007). Application of line sampling method to reliability benchmark problems. *Structural Safety* **29**: 208-221.

Rackwitz, R. (2001). Reliability analysis - a review and some perspectives. *Structural Safety* **23**(4): 365-395.

Rackwitz, R. and B. Fiessler (1978). Structural reliability under combined random load sequences. *Computers & Structures* **9**(5): 489-494.

Rosenblatt, M. (1952). Remarks on a Multivariate Transformation. *Annals of Mathematical Statistics* **23**(3): 470-472.

Schall, G., S. Gollwitzer and R. Rackwitz (1989). Integration of multinormal densities on surfaces. *Reliability and Optimization of Structural Systems' 88*, Springer**:** 235-248.

Schuëller, G. I., H. J. Pradlwarter and P. S. Koutsourelakis (2004). A critical appraisal of reliability estimation procedures for high dimensions. *Probabilistic Engineering Mechanics* **19**(4): 463-474.

Schuëller, G. I. and R. Stix (1987). A critical appraisal of methods to determine failure probabilities. *Structural Safety* **4**(4): 293-309.

Sindel, R. and R. Rackwitz (1998). Problems and solution strategies in reliability updating. *Journal of Offshore Mechanics and Arctic Engineering* **120**(2): 109-114.

Smith, A. F. M. and A. E. Gelfand (1992). Bayesian Statistics without Tears: A Sampling-Resampling Perspective. *The American Statistician* **46**(2): 84-88.

Straub, D. (2011). Reliability updating with equality information. *Probabilistic Engineering Mechanics* **26**(2): 254-258.

Straub, D. (2014). Engineering risk assessment. *Risk - A Multidisciplinary Introduction*. C. Klüppelberg, D. Straub and I. M. Welpe, Springer**:** 333-362.

Straub, D. and I. Papaioannou (2015). Bayesian Updating with Structural Reliability Methods. *ASCE Journal of Engineering Mechanics* **141**(3): 04014134.

Sudret, B. (2012). Meta-models for structural reliability and uncertainty quantification. *Fifth Asian-Pacific Symposium on Structural Reliability and its Applications (5APSSRA)*, Singapore.

Sundar, V. S. and C. S. Manohar (2013). Updating reliability models of statically loaded instrumented structures. *Structural Safety* **40**(0): 21-30.

Szabó, B., A. Düster and E. Rank (2004). The p-Version of the Finite Element Method. *Encyclopedia of Computational Mechanics*.